Robust superconductivity in quantum-confined Pb: Equilibrium and irreversible superconductive properties

Mustafa M. Özer,[1] James R. Thompson,[1,2] and Hanno H. Weitering[1,2]
[1]*Department of Physics and Astronomy, The University of Tennessee, Knoxville, Tennessee 37996, USA*
[2]*Materials Science and Technology Division, Oak Ridge National Laboratory, Oak Ridge, Tennessee 37831, USA*
(Received 29 June 2006; revised manuscript received 12 October 2006; published 15 December 2006)

Strong quantum size effects enable the formation of crystalline Pb films that are atomically flat on a *macroscopic* length scale. The superconducting properties of 5–18–monolayer-(ML) thick Pb films were investigated in a superconducting quantum interference device (SQUID) magnetometer using combined ac and dc methods. Even the thinnest films (5 ML) are extraordinarily robust type-II superconductors. Despite the extreme two-dimensional geometry, the thermodynamic parameters T_c and upper critical field H_{c2} are primarily controlled by the physical boundary conditions of the film and show no evidence for disorder-driven or fluctuation-driven quenching of superconductivity. A magnetically hard critical state is established as a consequence of vortex trapping by quantum growth defects.

DOI: 10.1103/PhysRevB.74.235427 PACS number(s): 74.78.−w, 68.55.Jk, 74.25.Qt

I. INTRODUCTION

Suppression of superconductivity in reduced dimensionality is a long-standing and thoroughly studied phenomenon. Fundamental understanding of the consequences of dimensional confinement for superconductivity is imperative for potential applications of superconductivity in tomorrow's nanoscale devices. Apart from the technological relevance of the subject, issues regarding formation, coherence, and robustness of quantum-confined Cooper pairs are intriguing academic questions.[1–5] The destruction of the ordered phase in two dimensions in principle proceeds via topological fluctuations of the Berezinskii-Kosterlitz-Thouless (BKT) type,[6–9] but the anticipated BKT transition is usually preempted by much stronger fluctuations, driven by enhanced Coulomb interactions in the presence of disorder.[10] Numerous experimental and theoretical studies of superconductivity in two–dimensional (2D) systems considered the normal-state resistance as the primary control parameter for tuning the pairing attraction.[11–17] For instance, it has been shown that superconductivity disappears in the ultrathin film limit when the resistance per square, $R_\square$, approaches $h/4e^2 = 6.45\ \mathrm{k}\Omega$, which is the quantum resistance for Cooper pairs.[13]

All of the above studies, with the exception of the high-T_c materials, have focused on quenched-condensed, high-resistivity films that are strongly disordered or granular in nature, emphasizing fluctuations in the amplitude or in the phase of the superconducting order parameter, respectively (sometimes referred to as the "fermionic" and "bosonic" mechanisms of T_c suppression, respectively[18]). In this study, we explore the superconductivity of *single-crystalline*, *low-resistivity* Pb films that are atomically flat on a *macroscopic*-length scale.[19] The unusual morphology and superior quality of the films can be attributed to the quantum nature of the film stability, as pointed out by several groups.[20–25] A recent study indicated possible oscillations in the superconductive transition temperature T_c, due to the quantum size effect in atomically smooth Pb films.[26,36] Here, we investigate the thermodynamic and nonequilibrium critical-state properties of significantly thinner films, ranging in thickness d from 5–18 monolayers (ML) where 1 ML=2.86 Å, which complements and expands our initial report[19] with additional data and in-depth analysis. The thermodynamic parameters T_c and upper critical magnetic field $H_{c2}(T)$ appear to be extraordinarily robust and are primarily affected by the thin-film boundary conditions. The robustness was also indicated by recent STM studies of the tunneling gap for flat-topped Pb islands.[27]

The quantum growth mode of these films naturally leads to the formation of nanoscale voids of atomically uniform 2 ML depth, which strongly pin the Pearl vortices in the film.[28,29] The observed, *macroscopic* critical currents of several $\mathrm{MA/cm^2}$ are quite comparable with the levels calculated from the known pinning geometry and superconducting length scales and imply an ideal Bean-type critical state.[29] Thus, both the thermodynamic and nonequilibrium superconductivity parameters of these high-quality films display an extraordinary robustness that is quite unexpected for low-dimensional geometries.

II. EXPERIMENTAL DETAILS

In this paper we study the various superconducting properties of ultrathin Pb films deposited on Si (111) substrates. After chemical cleaning with acetone, well-defined 7×7 reconstructed surfaces were obtained by flashing the samples to about 1470 K in ultrahigh vacuum (UHV). Pb was subsequently evaporated using a thoroughly degassed effusion cell. The deposition rates (~0.3 ML/min) were determined using *in-situ* x-ray photoemission spectroscopy (XPS) and *ex-situ* Rutherford backscattering spectroscopy (RBS). The crystalline structure of the films was verified by low-energy electron diffraction (LEED). If carefully executed, a reentrant bilayer-by-bilayer growth mode can be established at moderately low deposition temperatures, ranging from 200–250 K. This quantum growth mode is interrupted periodically by the growth of a single layer or trilayer.[22] The minimum thickness for smooth layer growth is 5 ML. In this

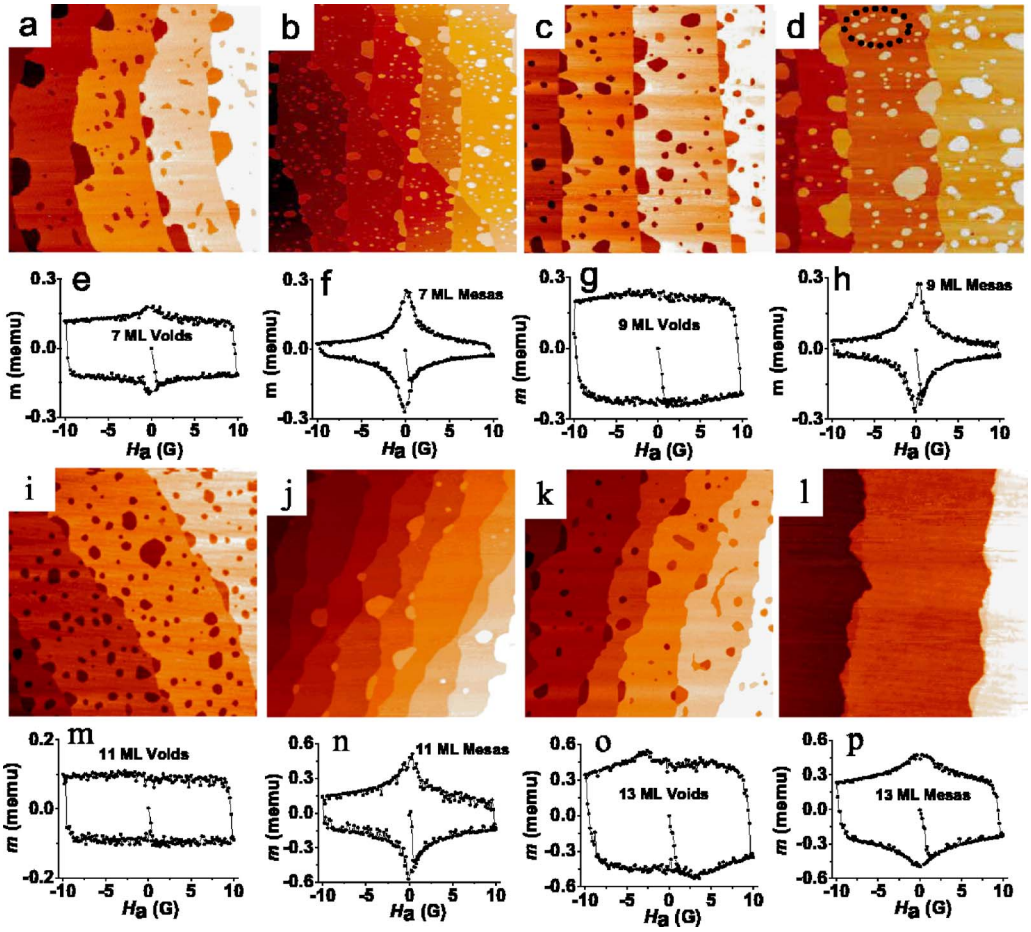

FIG. 1. (Color online) Scanning tunneling microscopy (STM) images of Pb films on Si(111) substrates; (a) ,(c) ,(i) ,(k) show 7, 9, 11, and 13 ML films with voids (slightly underdosed) with corresponding magnetization loops (e), (g), (m) ,(o). The same thicknesses with voids (overexposed) are shown in (b) ,(d), (j), (l)) with corresponding magnetization loops (f), (h), (n), (p). All STM images measure about 700×700 nm^2; dc magnetic signals are for samples at $T=2$ K with lateral area of 3×3 mm^2 [except for (n), 11 ML with mesas, whose area is 6×3 mm^2].

study, we have thicknesses $d=5$, 7, 9, 11, 13, 14, 16, and 18 ML. (For the [111] direction in Pb, 1 ML=0.286 nm.) This layer count excludes the wetting layer which is known to be 1 ML.[30,31] A small excess amount of Pb, i.e., $(N+\varepsilon)$ ML, produces 2 ML nanomesas on top of an otherwise smooth N-layer film; small deficits of Pb generate 2-ML-deep nanovoids. Figure 1 shows STM images of 7, 9, 11, and 13 $(\pm\varepsilon)$ ML thin films, which reveal the presence of nanovoids and nanomesas, respectively. The metastable morphology of the Pb films and its chemical integrity were protected by depositing a $\sim$0.1-μm-thick capping layer of amorphous Ge at $\sim$100 K substrate temperature, prior to their removal from UHV. The morphological stability of the capped layers at room temperature was verified with STM and will also be evident from the thickness-dependent T_c data.

The superconductive properties of the films were measured inductively as a function of temperature and perpendicular magnetic field, using a SQUID magnetometer (Quantum Design model MPMS-XL). Both reversible (i.e., the superconducting transition) and irreversible (magnetic hysteresis) properties of the samples were investigated employing collinear dc+ac magnetic fields. This contactless method eliminates the need for a conductive capping layer and has the additional advantage that it avoids potential changes in physical properties, e.g., via a proximity effect introduced by metal contacts or metallic capping layers.[26] Furthermore, the inductive determination constitutes a more stringent criterion for the existence of macroscopic supercurrents (obtained from a macroscopic magnetic moment), as opposed to dc transport measurements, which merely detect the onset of a filamentary supercurrent path. For ac studies, a small 100 Hz ac probing field was superimposed parallel to a dc field. These external fields generate circulating screening currents and an associated magnetic moment m. The ac moment $m=m'-im''$ contains a diamagnetic in-phase term and a lossy, out-of-phase component. Figures 2 and 3 are examples of the ac magnetic moments at different dc fields and different ac amplitudes, respectively, for a 9 ML film with voids. Full Meissner-type screening implies $m'=-(4\pi)^{-1}(1-D)^{-1}HV$, where V is the film volume and H is the applied magnetic field. Hence the initial diamagnetic response is amplified by a factor $(1-D)^{-1}$, where the demagnetization factor $D\approx1$ for a thin film in perpendicular magnetic field. Assuming that the square samples act as a thin disc with radius $r\approx1.5$ mm and

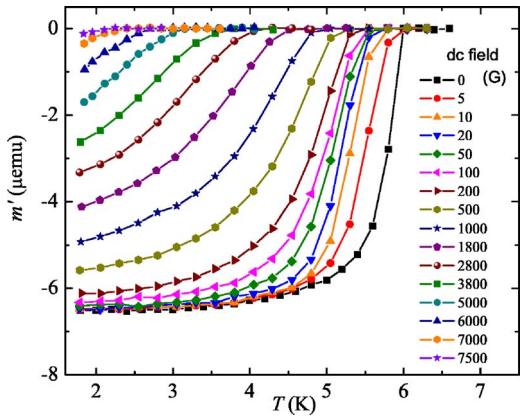

FIG. 2. (Color online) Real part m' of the ac magnetic response of a 9 ML Pb film with voids, measured in various dc fields. All curves employ an ac probing amplitude of 10 mG superimposed on the dc fields shown in the legend (the superconducting onsets shift from high to low temperature). The shift of the superconductive onset with applied dc magnetic field delineates the $H_{c2}(T)$ phase boundary.

thickness d, the susceptibility corresponding to the maximum screening is given (in dimensionless cgs form) by[32] $-4\pi\chi_{\max}=8r/3\pi d$, which is in excellent quantitative agreement with the measured SQUID signal shown in Fig. 4. By varying the temperature and applied dc fields, we obtain T_c, $H_{c2}(T)$, and the critical current density $J_c(T,H)$, as discussed below.

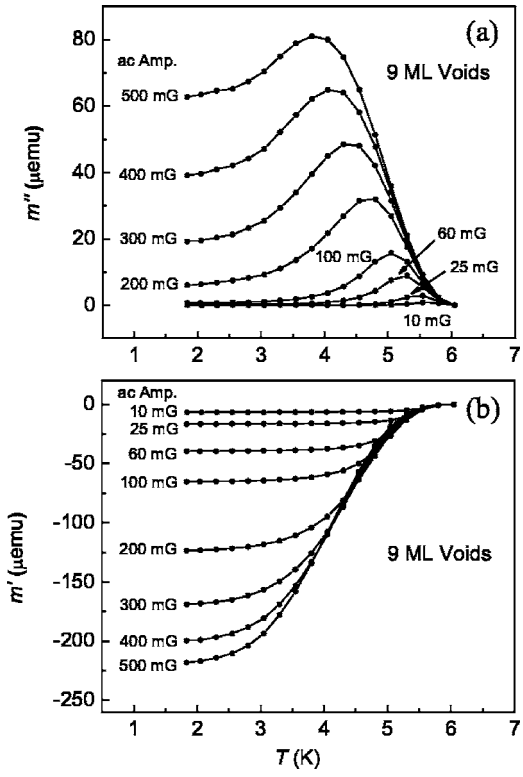

FIG. 3. (a) Imaginary part m'' of the ac magnetic response of a 9 ML Pb film with voids, measured in a 5 G dc field (perpendicular to the film plane) using various probing amplitudes of the collinear 100 Hz ac field. (b) Corresponding real signal m' plotted vs temperature as above.

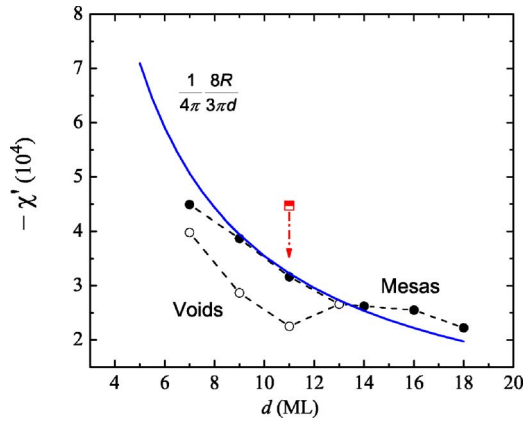

FIG. 4. (Color online) Maximum ac susceptibilities of 3 $\times$ 3 cm^2 under- and overexposed (overdosed) samples measured at 1.8 K with only 10 mG ac amplitude (0 G dc). The solid curve shows the calculated full-screening values assuming circular samples with 3 mm diameter. The analytical expression is taken from Clem and Sanchez.[32] For the larger 11 ML sample with voids, the as-measured value of χ' (square) has been scaled down by a factor of $[(3\text{ mm}\times 3\text{ mm})/(6\text{ mm}\times 3\text{ mm})]^{1/2}$ to compensate for its larger demagnetizing factor.

III. RESULTS AND DISCUSSIONS

A. Equilibrium properties

Lead, ordinarily a type-I superconductor in bulk form, takes on type-II behavior[33,34] below a critical thickness of $\sim$250 nm.[35] This critical thickness significantly exceeds our film thicknesses. In the following, we first consider the equilibrium properties of these ultrathin films. Later, we will show how their unique morphology controls the currents and vortices in these materials. The filled squares in Fig. 5 show the superconductive transition temperature T_c plotted as a function of $1/d$. The T_c data are obtained from the onsets of the in-phase ac response using a 10 mG probing amplitude [Fig. 5 (inset)]. The T_c values of the $(N\pm\varepsilon)$ ML Pb films with mesas or with voids are identical to within 0.1 K. The solid line is a linear fit to the data that nicely extrapolates to the bulk T_{c0} (7.2 K) at infinite thickness. Hence this linear behavior can be expressed as

$$T_c(d) = T_{c0}(1 - d_c/d). \tag{1}$$

The "critical thickness" d_c for the appearance of superconductivity is 1.5 ML. This suggests that a single bilayer of Pb should still sustain superconductivity. Note that the interfacial wetting layer (1 ML thickness) is excluded in this layer count. If the wetting layer were included, the $1/d$ plot would no longer extrapolate to the correct bulk T_{c0}, which suggests that the wetting layer does not play a substantial role in superconductivity.

Figure 5 also includes the T_c data from Guo *et al.*[26,36] The latter values are consistently lower than the present data and do not extrapolate to the correct bulk T_{c0}, suggesting an in-

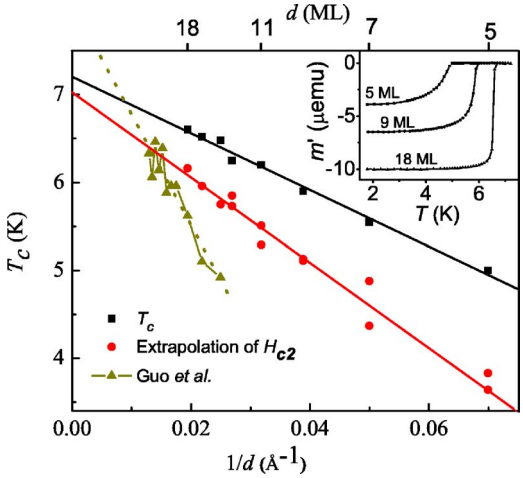

FIG. 5. (Color online) T_c data indicated in the legend are obtained from the onset of real ac magnetization taken with 10 mG probing amplitude as exemplified in the inset for some film thicknesses. T_c values scale linearly with $1/d$ and extrapolate to bulk value (7.2 K) in the thick film limit. T_c^* values are obtained by extrapolating the linear part of $H_{c2}(T)$ to zero dc field, as illustrated in Fig. 6. Extrapolating $T_c^*(d)$ to $1/d=0$ gives a value of (6.96±0.13 K), which is about $1\frac{1}{2}$ standard deviations below the T_c of bulk Pb. Data of Guo *et al.*[26,36] show oscillations in T_c in the layer-by-layer growth regime, which is accessible only for thicknesses above about 20 ML.

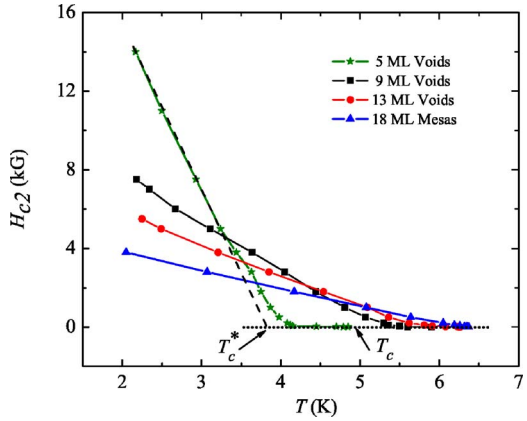

FIG. 6. (Color online) $H_{c2}(T)$ values are obtained from the onset of diamagnetic screening in various dc fields, measured using a 10 mG ac amplitude as illustrated in Fig. 2. Due to systematic rounding of H_{c2} values near T_c, the linear parts of the H_{c2} curves do not extrapolate to T_c, but rather to a new set of characteristic temperatures denoted as T_c^*; the extrapolation is shown for a 5 ML film.

fluence of the Au capping layer used in that study or some other effect. Notice the quantum oscillations in $T_c(d)$ (Refs. 26 and 36) that are superimposed on the overall $1/d$ falloff in the plot. While a $1/d$ variation of $T_c(d)$ has been observed in many thin-film systems, the film smoothness and accuracy of the layer thickness in the present study are clearly unprecedented. The lowering of T_c in thin films was originally interpreted in terms of a BKT transition[6–8] while later reports emphasized the role of enhanced pair-breaking Coulomb interactions in the presence of strong disorder.[10,37,38] Using the direct proportionality between the mean- free path l and film thickness that will be shown in the next section, we can rule out both scenarios. Specifically, the BKT and pair-breaking mechanisms predict that to first order $\Delta T_c(d)=T_{c0}-T_c(d)$ should be proportional to $R_\square(d)$. Our Pb films are highly ordered. Their sheet resistance can be estimated from the relation for Pb that[39] $\rho\times l=1.5\times 10^{-11}\ \Omega\ \mathrm{cm}^2$; the sheet resistance then follows from ρ and layer thickness d. For the thinnest film (5 ML), $R_\square$ is only ~200 Ω, as estimated from the mean-free path. These values are consistent with normal-state properties of ultrathin Pb films determined by Vilfan *et al.*[40] This low resistance would not only produce a negligible $\Delta T_c(d)$ for the BKT scenario, but it also lies far below the critical resistance of the superconductor-insulator transition in the pair breaking scenario.[13] In addition, according to Ref. 40, the normal-state conductivity $\sigma_{2D}\propto d$ meaning that $R_\square(d)$ and hence $\Delta T_c(d)$, should be proportional to $1/d^2$ instead of the observed $1/d$ dependence. The Finkelstein theory for pair breaking in low dimensionality[37] also does not reproduce the correct thickness dependence.

Simonin[41] provided an alternative explanation for the $1/d$ dependence of T_c by explicitly including a surface term in the three-dimensional Ginzburg-Landau (GL) free energy. This essentially modifies the boundary condition for the superconducting order parameter in thin films, predicting that $T_c(d)=T_{c0}[1-2C\xi^2(0)/d]$. Here, $\xi(0)$ is the coherence length at $T=0$ K and C is a constant whose microscopic origin is related to the electron-phonon coupling strength and density of states in the bulk. Our data qualitatively agree with this phenomenological model although it should be realized that the explicit expression for C and the resulting expression for critical thickness d_c are oversimplified.[41] In particular, the experimental values of d_c are considerably smaller than those expected from the Simonin theory.

Figure 6 shows representative $H_{c2}(T)$ data in perpendicular fields that were obtained from the onset temperatures of m' in the presence of a dc magnetic field, as illustrated in Fig. 2. At low temperatures $H_{c2}(T)$ varies nearly linearly with temperature, conforming to the standard $(1-T/T_c)^{-1/2}$ dependence of the GL coherence length.[29] Two observations are very striking. First, the slope of $H_{c2}(T)$ versus T increases systematically for decreasing film thickness. As will be shown in Sec. III B, this can be fully attributed to boundary scattering. Secondly, $H_{c2}(T)$ markedly flattens near T_c resulting in a characteristic "knee profile," which is particularly noticeable for the thinner films. The knee profile is much less apparent at 18 ML, which is also the reason why it has not been noticed in previous studies of films with thicknesses greater than 18 ML.[36] This "knee" feature directly reflects the large shifts in the $m'(T,H)$ data produced by the application of a small dc field, as is evident in Fig. 2. This behavior of $H_{c2}(T)$ is reminiscent of that in superconductive normal-metal multilayers. For such systems, Takahashi and Tachiki[42] showed theoretically that a similar "knee" structure arises when the temperature-dependent $\xi(T)$ becomes comparable with some T-independent length scale L (e.g., a layer thickness). Subsequently, Gvozdikov[43] showed that a knee structure could also arise in a *thin film* exhibiting structural inhomogeneities with locally elevated T_c. For our Pb films, the length scales L may be associated with distances between

scattering centers (which reduce ξ and elevate H_{c2}). For instance, L could be the average terrace size in the substrate, or the size of (or separation between) the nanomesas or nanovoids, etc. While this conjecture provides qualitative understanding of the low slope of H_{c2} near T_c and the scattering-enhanced H_{c2} at lower temperatures, further theoretical development is clearly needed.

One theoretical constraint comes from the fact that, in the current data, the knee profile is directly correlated with the film thickness. Extrapolation of the linear $H_{c2}(T)$ segments to zero dc field produces a set of extrapolated GL temperatures $T_c^*(d)$ as illustrated in Fig. 6. Most remarkably, $T_c^*(d)$ as well as $T_c(d)$, and hence $\delta T_c(d)=T_c(d)-T_c^*(d)$, *all* scale linearly with $1/d$ as demonstrated in Fig. 5. An alternative interpretation for the existence of a T_c^* would be that $T_c^*(d)$ could perhaps be interpreted as an extrapolated GL or "mean-field" superconducting transition temperature, implying that the region between $T_c^*(d)$ and $T_c(d)$ should be dominated by fluctuations. As will be shown below, macroscopic critical currents can still flow in the T region between T_c and T_c^*, which greatly reduces the likelihood of explanations based on fluctuations or flux-melting scenarios. Moreover, we estimated the width of the possible fluctuation region in thin Pb by evaluating the 2D Ginzburg number $G_i=\delta T_c/T_c$ using the expression derived by Bulaevskiĭ *et al.*[44] The resulting values of δT_c are smaller than the observed $\Delta T_c(d)$ by at least one order of magnitude. In addition, inserting the mean-free-path result $l(d)\cong 2\times d$ into the Bulaevskiĭ expression again implies that $\delta T_c \propto 1/d^2$, rather than the observed $1/d$ dependence. Specifically, the magnitude and thickness dependence of δT_c of these low-resistivity, crystalline thin films cannot be accounted for within the bosonic or fermionic fluctuation scenarios of T_c suppression,[10,37,38] nor can it be explained by involving mesoscopic fluctuations.[18] Finally, we did not observe a qualitative agreement between our data and the 2D flux-line melting theory[45] because the curvature of H_{c2} near T_c should then be opposite to what we observe.

B. Length scales

Having discussed the equilibrium properties of the ultrathin lead films, we now consider the fundamental length scales (obtainable from a variety of magnetic studies[46]), as they will be needed later to evaluate the nonequilibrium critical-state properties. While the type I-type II crossover in thin films is fundamental and does not require an altered Ginzburg-Landau parameter,[47] $\kappa=\lambda/\xi$, the fundamental length scales in these Pb films are significantly affected by the 2D geometry. For instance, the dominant role of surface scattering in the ultrathin limit reduces the GL coherence length ξ_{GL} significantly below the BCS value of bulk Pb, $\xi_0^{bulk}=905$ Å. Values for $\xi_{GL}(T)$ were obtained from upper critical-field data via the relation $H_{c2}(T)=\Phi_0/2\pi\xi_{GL}^2(T)$, where Φ_0 is the flux quantum.[29] $H_{c2}(T)$ was measured down to 1.8 K as illustrated in Fig. 6. Values of H_{c2} at $T=1.8$ K are shown in Fig. 7 for all thicknesses studied. For a 9 ML Pb film with voids, $\xi_{GL}(1.8\text{ K})\approx 200$ Å, which is reduced significantly from the value of bulk Pb. The reduction in ξ_{GL} is attributed primarily to the small electronic mean-free path

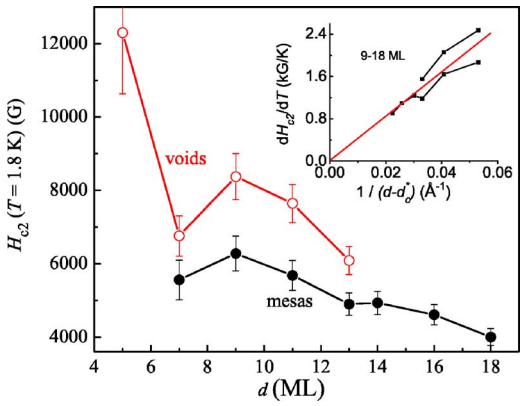

FIG. 7. (Color online) The upper critical field H_{c2} at base temperature (1.8 K) plotted vs film thickness d. The inset shows the slope of H_{c2} curves in the linear regime, plotted as a function of $(d-d_c^*)^{-1}$ (see the text).

$l(d)$. Disorder in the interfacial wetting and possibly the capping layers is most likely the dominant contributor to the scattering rate. From the "full-value" expression,[48]

$$\xi_{GL}(d)=0.739[\xi_0^{-2}+0.882(\xi_0 l)^{-1}]^{-1/2}(1-T/T_c)^{-1/2}, \quad (2)$$

we obtain $l(d)$ at 1.8 K for all materials. These values are plotted in Fig. 8, showing that $l(d)\cong 2\times d$. These values are somewhat smaller than those given in Ref. 19, which were calculated using extrapolations of H_{c2} to 0 K. Alternatively, they are significantly larger than the mean-free paths $l\approx 0.5\times d$ inferred from Bao *et al.*[36] from their upper critical-field data and, independently, from their resistivities using the $\rho\times l$ product of Strongin *et al.*[39] Note that we find $l(d)$ to be systematically smaller for the films with voids as compared to those with mesas. The linear fit in Fig. 8 was not forced to pass through zero. For calculating $l(d)$, the BCS coherence length ξ_0' has been renormalized to account for the lower T_c in thin films, using[48] $\xi_0' T_c^{film}=\xi_0^{bulk} T_c^{bulk}$. Our mean-free-path estimates are slightly smaller than those of Vilfan and co-workers from normal-state transport measurements.[40]

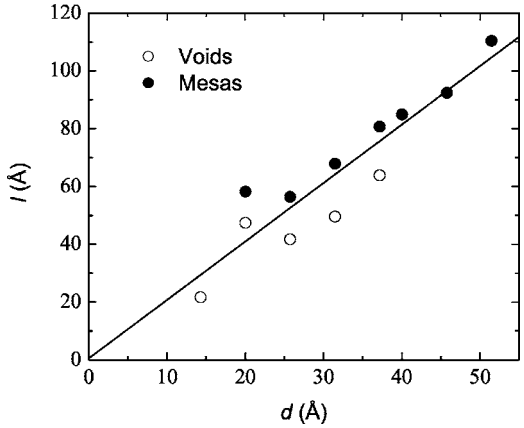

FIG. 8. Electronic mean-free path (mfp) values obtained from the full value expression (Ref.48). Eq (2). The mfp for a film with voids is always smaller than that with mesas. The straight line is an unconstrained linear fit to the data.

These authors find that $\sigma \propto d$, and consequently $R_\square \propto 1/d^2$, similar to our findings.

According to the Anderson theorem,[49] the product $\lambda\xi$ should be independent of scattering and thus independent of the film thickness; consequently $\lambda_{eff}\xi_{GL} \approx \lambda_L \xi_0'$, where λ_L is the London penetration depth of bulk Pb (~370 Å). For a 9 ML film we obtain a scattering-increased penetration depth $\lambda_{eff} \approx 1500$ Å so that $\kappa = \lambda/\xi \approx 5$. Finally, the 2D screening distance for a thin film in a perpendicular magnetic field is $\Lambda \equiv 2\lambda_{eff}^2/d$; the length Λ can be interpreted as the lateral radius of a "Pearl vortex,"[28,29] which could exceed the sample dimensions (3×3 mm^2) for very thin films sufficiently close to T_c.[50]

Finally, let us consider the thickness dependence of H_{c2} in Fig. 7. The findings above can be used to explain the overall systematic thickness dependence of H_{c2} in the GL regime, using the combined effects of the $1/d$ variation of $T_c^*(d)$ and a mean free path limited by boundary scattering. Using Eq. (1), it can be shown that $-dH_{c2}/dT$ should be proportional to $(d-d_c^*)^{-1}$ as is indeed observed experimentally in the inset to Fig. 7. Here, $d_c^* \cong 2.4$ ML is the thickness where $T_c^*(d)$ extrapolates to 0 K. In addition to the overall falloff of H_{c2} with thickness, the data in the main panel of Fig. 7 also exhibit some structure, with local minima near $d=7$ and 13 ML. This structure may reflect the 9 ML "beating period" of properties in quantum confined films of pure Pb,[51] although the present data are not extensive enough to provide a definitive demonstration of this phenomenon. To conclude this section, the thermodynamic parameters T_c, T_c^*, and $H_{c2}(T)$ of high-quality Pb films are primarily determined by the boundaries of the film and thus display a robustness that is quite unexpected for low-dimensional geometries.

C. Nonequilibrium critical-state properties

The nonequilibrium properties of the Pb films are also remarkably robust. Figure 1 shows the dc magnetization loops at $T=2$ K for underdosed 7, 9, 11, and 13 ML films with 2-ML-deep voids and those of the overdosed films with 2-ML-tall mesas. The contrast between the two cases is striking, consistently showing hard, nearly rectangular hysteresis loops for the films with voids and soft hysteresis loops for the films with mesas. From the highly irreversible magnetization of the film with voids, we conclude that those films are almost ideal Bean-type[52,29] superconductors at low temperatures, due to the exceptionally strong vortex pinning by the nanovoids. Their areal density N_A is estimated to be $\sim 2.6 \times 10^{10}$ cm^{-2} and the diameter of the blind holes is comparable to ξ_{GL}. By attaching one flux quantum Φ_0 per void, one obtains a "matching field" $B_\Phi = N_A \times \Phi_0 \cong 5500$ G, meaning that the pinning array is strongly underfilled at a low dc field. From the dc magnetization, the critical-current density was calculated using the critical-state relation $J_c = 30m/Vr$ where m is the measured magnetic moment, V is the volume of the film, and r is the macroscopic radius of the sample (≈1.5 mm). This yields $J_c = 2.0$ MA/cm^2 for the underdosed 9 ML film at 2 K in a 5 Oe dc field. With increasing temperature, the hysteresis in the magnetization loops decreases progressively, as shown in Fig. 9 for a 9 ML film

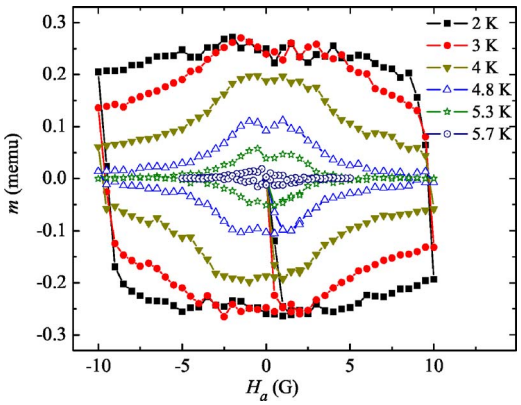

FIG. 9. (Color online) Magnetization loops for a 9 ML quantum confined Pb film with voids, measured at temperatures well below $T_c^* = 5.1$ K, near it and above T_c^*; for this film, $T_c = 5.9$ K.

with voids. For T approaching T_c^* and beyond, the decrease is particularly pronounced, as the coherence length ξ (and penetration depth λ) increase rapidly; this means that vortex pinning becomes weaker, as discussed later in this section.

For the overdosed films, the application of small dc fields quickly depresses the magnetization, even at low temperatures well below T_c^* as seen in the data at 2 K in Fig. 1. This indicates that the areal density of *effective* pinning centers in these materials is too small to accommodate even a modest density of vortices. While voids attract vortices and pin them, mesas repel them, meaning that generally, vortices can move and dissipate energy by simply avoiding the mesas. In some cases though, repulsive interactions can localize vortices, thereby pinning them. One such special case arises when several mesas form a circular "corral" (or cage) that can trap flux inside; see, for example, the top center portion of Fig. 1(d). The area density of "corrals" is expected to be quite low, however, so this pinning mechanism will be effective only for very small magnetic fields near $H=0$. Indeed, this caging effect explains a curious feature in the dc magnetization loops in Fig. 1, that the magnetic moments with either voids or mesas are often comparable at a field very near zero: with low enough density, all vortices can be pinned, but the application of a small dc field quickly exhausts the supply of "corral" pinning sites.

The critical-current density J_c was also determined from the ac magnetic response. It follows from the critical-state model that J_c can be calculated from the peak position of the imaginary ac susceptibility (Fig. 3) using $J_c = 1.03 H_{ac} d^{-1}$, where H_{ac} is the peak amplitude of the applied ac modulation field.[32] Accordingly, we have measured χ'' in various ac +dc fields as shown in Fig. 3, to obtain a complementary set of $J_c(T,H)$ values. Within the resolution of the measurement, the onset of χ'' signaling dissipative irreversible magnetization always coincides with the onset of diamagnetic screening χ'. This indicates that the thermodynamic $H_{c2}(T)$ phase boundary coincides with the onset of irreversible magnetization. Notice that the formula $J_c = 1.03 H_{ac} d^{-1}$ does *not* include the sample volume. The general consistency between the J_c values from ac susceptibility (2.8 MA/cm^2) and dc magnetization (2.0 MA/cm^2) thus indicates that the critical currents are truly macroscopic. For instance, if the sample were

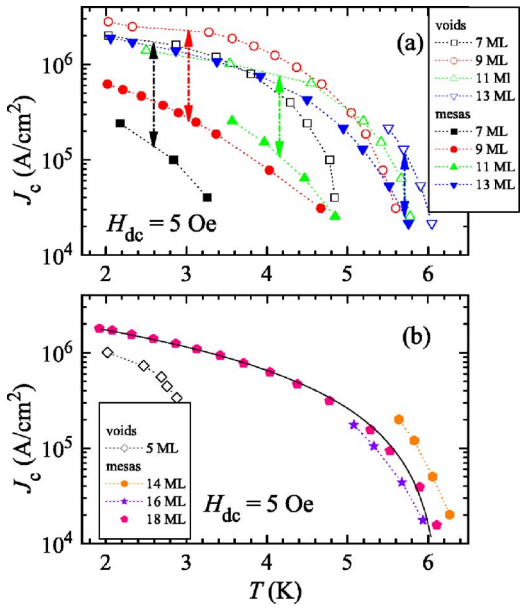

FIG. 10. (Color online) Critical-current density J_c in perpendicular dc magnetic field $H=5$ Oe, as obtained from the peak positions of the imaginary ac magnetization curves using $J_c = 1.03 h_{ac} d^{-1}$. (Note that for each ac amplitude, one only obtains the J_c value at the temperature where χ'' is maximum. J_c values for other temperatures were calculated from the other $\chi''(T)$ values using the analytical results of Clem-Sanchez[32] for a Bean-type superconductor.) Part (a) contrasts J_c in films containing voids or mesas, for thicknesses $d=7$, 9, 11, and 13 ML; voids give stronger pinning and higher J_c in every case. In (b) are shown results for other thicknesses, also with semilogarithmic axes. For the 18 ML film, the solid line is fitted to a 3/2 power-law dependence on temperature, as described in the text.

subdivided into $N \times N$ disconnected superconductive domains, then the dc measurement would produce J_c values smaller by a factor of $1/N$. In fact, this macroscopic nature of the screening response was already evident in Fig. 4, where it is shown that m' corresponds to maximum diamagnetic screening. Hence the ~ 2 MA/cm^2 critical currents follow a macroscopic trajectory along the sample's circumference, despite many surface imperfections such as atomic steps on the substrate. For a 9 ML film, these current densities imply circulating macroscopic supercurrents of order 100 mA.

In Fig. 10 we show the critical currents obtained from ac+dc measurements as a function of temperature for various film thicknesses at a 5 G dc field. Examination of Fig. 10(a) shows that films with mesas have J_c values that are smaller by a factor of 10 — 4 at all temperatures, compared with those with voids: the ac values are larger with $d=7$, 9, 11, and 13 ML, respectively, i.e., in every case where both defect morphologies were available. This finding is consistent with the observation of magnetically soft loops in the dc measurements. (Also, it shows that the anomalously low dc moment in Fig. 1(m) is an artifact, likely due to interruptions in the current path near the edges of this sample.) We estimate the depairing current density of our films using $J_d \approx H_c/\lambda_{eff} \cong 20$ MA/cm^2 (for a 9 ML film with voids). This result indicates that the critical currents in the thin-film superconductors reach $\sim 10\%$ or more of the theoretical depairing current density, which is extraordinarily high. This observation is further illustrated by a simple model calculation, as shown below.

The scale of the vortex line energy per unit length is given by[29] $\varepsilon_0 = \Phi_0^2/(4\pi\lambda_{eff})^2$. The 2 ML depth of the voids amounts to a significant percentage of the total film thickness, which in turn implies that voids must act as trapping centers of the Pearl vortices. Because the uniform depth of the quantum defects can be thought of as a segment of a columnar defect or "blind hole," the critical-current density can be estimated from a slightly modified expression of Nelson and Vinokur:[53]

$$J_c = [c\Phi_0/(4\pi)^2 \lambda_{\text{eff}}^2 \xi](\Delta d/d), \tag{3}$$

where c is the speed of light and $\Delta d = 2$ ML is the depth of the pinning center. Estimating J_c from this expression gives a value of about 4 MA/cm^2 for the 9 ML film at low temperatures and indicates a pinning energy $U_0 = \varepsilon_0 \Delta d$ of ~ 500 K. The experimental ac measurement of J_c is ~ 2.8 MA at low temperatures, which compares quite well with the calculated value. Furthermore, the temperature dependence of the critical-current density with voids follows the relation $J_c(T) \propto (T_c^* - T)^{3/2}$ in the GL regime below T_c^*, as shown earlier.[19] This is fully consistent with the expected $(T_c^* - T)^{-1/2}$ variation of λ_{eff} and ξ in GL theory. We find that $J_c(T)$ in films *with mesas* also is well described by the same 3/2 power law, as illustrated in Fig. 10(b) for an 18 ML film with mesas; the solid line shows this temperature dependence fitted to the data and yielding $T_c^* = 6.18$ K in coincidence with the value from $H_{c2}(T)$ in Fig. 5. This similarity in temperature dependencies is consistent, of course, with the approximately parallel curves in Fig. 10 for films of equal thickness.

According to Eq. (3), vortex pinning by voids should fall off with thickness due to the $1/d$ factor, combined with variations in $\lambda_{eff}(d)$ and $\xi(d)$. Increasing the film thickness, however, also permits a greater number of other defects, e.g., pointlike defects such as vacancies and interstitials, to contribute to vortex pinning for both film types. As a consequence of these two considerations, the contrast in J_c between films with voids and mesas tends to diminish for thicker films, as is evident in Fig. 10.

Before continuing, let us consider more closely pinning in the materials shown in Fig. 1, where there are voids of varying radii. Consider the theoretical origin of Eq. (3), an expression for the *maximum* critical-current density supported by columnar defects, with noninteracting vortices. For a columnar defect with radius c_0, Mkrtchyan and Shmidt[54] and Blatter *et al.*[9] obtained expressions for the pinning energy per unit length U_0' in limits that the coherence length ξ is either large or small compared with c_0. From these, Nelson and Vinokur generated a formula interpolating between those limits, with $U_0' \approx \frac{1}{2}\varepsilon_0 \ln[1 + c_0^2/2\xi^2]$. The maximum restoring force provided by this potential determines the J_c in bulk materials. For our thin films with voids of various radii, we see that the pinning energy and associated J_c depends only weakly—logarithmically—on the radius of the void, provided there are many voids with radii $\gg \xi$ as we have. Consequently, variations in void size have only a secondary ef-

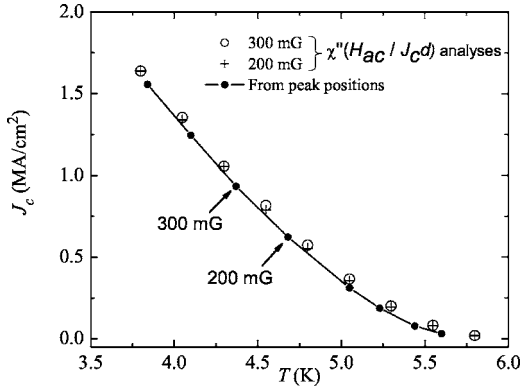

FIG. 11. Critical-current densities obtained from either the peak positions of the imaginary magnetization, or from the calculations[32] according to Clem and Sanchez—all for a 9 ML film with voids—in dc field $H=5$ Oe. Two independent J_c calculations using the 200 and 300 mG data are shown.

fect on pinning and J_c, particularly in comparison with the profound difference (attractive versus repulsive interactions) between voids and mesas, respectively.

Within the critical-state model, the relation between χ' and χ'' can be calculated [32] as a function of $2H_{ac}/J_c d$. This relation makes it possible to interpolate the J_c values between the discrete J_c values that were obtained from the peak positions in χ'' (Fig. 3). It furthermore allows us to extrapolate J_c outside our measurement range. Figure 11 shows a set of J_c values obtained in this manner.

The demarcation between loss-free current flow and dissipative conduction in a superconductor can be parametrized using the power-law exponent n in the current-voltage relation $E=E_c(J/J_c)^n$ (E is the electric field).[32,55] The Bean model implies perfect loss-free currents with $n=\infty$, while ohmic transport implies $n=1$. The relation between χ' and χ'' can be calculated theoretically for different values of n. Hence, n can be estimated by comparing the experimental (χ',χ'') relation with the theoretical relations for different n. Indeed, the (χ',χ'') values obtained from the ac response nicely collapse onto the Cole-Cole diagram of the Bean critical state ($n=\infty$), as shown in Fig. 12(a) for 9 ML film with voids. These data include all the (χ',χ'') pairs measured between 1.8 K and T_c, at a 5 G dc field with ac amplitudes ranging from 200 to 1100 mG. Data that are measured with ac amplitudes below 200 mG significantly deviate from the collapsed Cole-Cole data, which will be discussed later. The maximum of the Cole-Cole plot is located at $\chi''\cong 0.245$, in excellent agreement with the theoretical maximum of a Bean-type critical state for a thin disk, which gives $\chi''\cong 0.241$.

Cole-Cole plots for various dissipation mechanisms were calculated by Shantsev *et al.*[56] Comparison between the collapsed Cole-Cole data in Fig. 12(a) and theoretical Cole-Cole plots for finite creep exponents[55] indicate that $n>100$. This conclusion of very large n value was verified independently by real-time measurements of the current decay rate, as discussed below in Sec. III D. Qualitatively, the Cole-Cole plot for the film with mesas in Fig. 12(b) exhibits a pronounced deviation from the ideal Bean curve, compared with the film

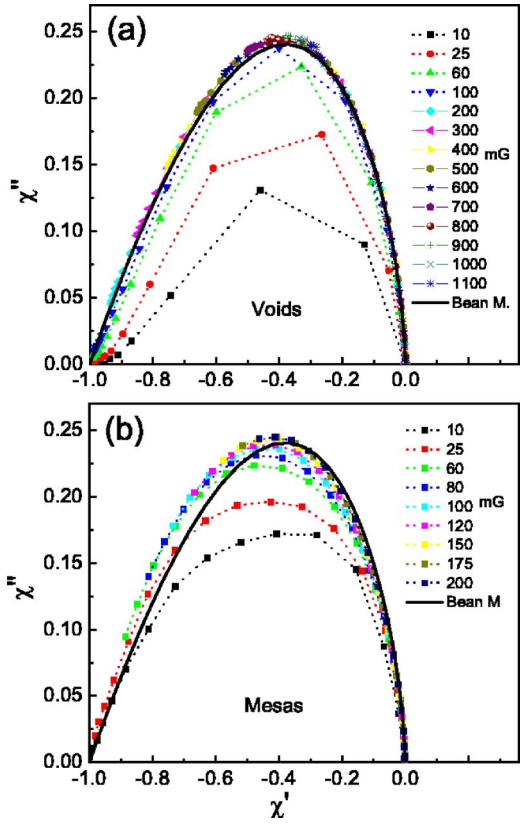

FIG. 12. (Color online) Cole-Cole plot of χ'' vs χ' for 9 ML films—(a) with voids and (b) with mesas—all measured in a 5 G dc field using many different ac field amplitudes, as shown. Solid curves correspond to the ideal Bean case.

with voids; the shift of the peak toward more negative values of χ' is consistent with the weaker pinning[56] and softer hysteresis loops in the material with mesas.

As noted, small ac amplitudes give experimental maxima of χ'' that fall well below the Cole-Cole curve for the Bean model. To delineate this effect, Fig. 13 shows the observed maximum of χ'' as a function of the ac field amplitude for 9 ML films. It is likely that the reduced dissipation at low H_{ac} arises from "elastic motion" of the vortices in the Campbell

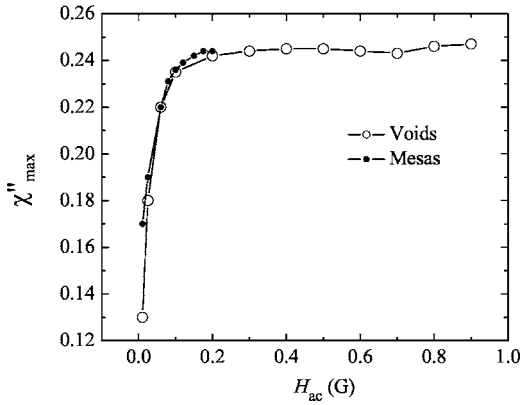

FIG. 13. Maximum value of χ'' attained, plotted as a function of the applied ac probing amplitude. Samples are 9 ML films with either voids or mesas, in an applied dc field of 5 G.

regime[57] in which the low driving force is too weak to depin vortices. At very low ac fields, the force on the vortices is proportional to their *elastic* displacement. The associated Meissner-type, nondissipative currents serve to screen the film and restrict the loss (χ''_{max}) to levels below that obtained in a strictly Bean-type critical state. Qualitatively similar reductions in (χ''_{max}) were observed in low ac fields by Pasquini *et al.*[58](and references therein) in thin films of the high-T_c superconductor $YBa_2Cu_3O_7$; these researchers successfully analyzed their findings in terms of a high-screening, low-dissipation Campbell regime at low amplitudes. Also, Herzog *et al.*[59] observed an amplitude dependence similar to that in Fig. 13 (with, however, a small but experimentally significant continuing increase in (χ''_{max}) in larger fields H_{ac}). These authors too attributed the low-field falloff in χ''_{max} to an "increased dominance of screening rather than a change towards a different loss mechanism." Given the marked differences in their J_c values, it is curious that the films with voids and mesas behave so similarly in Fig. 13; it may be that the difference between two morphologies is irrelevant for the weak driving forces at low ac amplitudes.

D. Flux creep

Lastly, let us consider the time dependence of the critical-current density or "flux creep." In order to measure the decay rate of the critical currents without potential measurement artifacts, the sample was held stationary during the measurements. To begin, we quickly moved the sample from a position with low field (8 cm below the center of the magnet) into a higher-field region at the center of the SQUID pickup coils, where $H=5$ Oe. This induces the critical state. The sample was then kept stationary as the SQUID signal (linearly related to the dc magnetic moment $m \propto J$) was monitored over time.[60] The resulting data were analyzed according to the relation

$$J(t) = J_0 - J_1 \ln(1 + t/\tau), \tag{4}$$

where τ is an initial transient time.[61] Here,

$$J_1 = \frac{\partial J(t)}{\partial \ln(t)}, \tag{5}$$

and

$$\tau = 0.41 \frac{J_1 d}{dH_a/dt}. \tag{6}$$

Equation (4) describes the signal decay reasonably well, as illustrated in Fig. 14 for data at $T=2.5$, 3.5, and 4.5 K. The normalized creep rate S then follows from

$$S = \frac{1}{J_c} \frac{dJ}{d \ln(t)} \cong \frac{J_1}{J_0} = \frac{T}{U_0}, \tag{7}$$

where the last equality comes from standard Anderson-Kim theory for flux creep and U_0 is the vortex pinning energy. The resulting values for S are shown in the inset of Fig. 15. Using the relation[62] for the power-law exponent $n=1+S^{-1}$, we obtain independently that $n \sim 100$, in good agreement with conclusions from the Cole-Cole analysis. According to

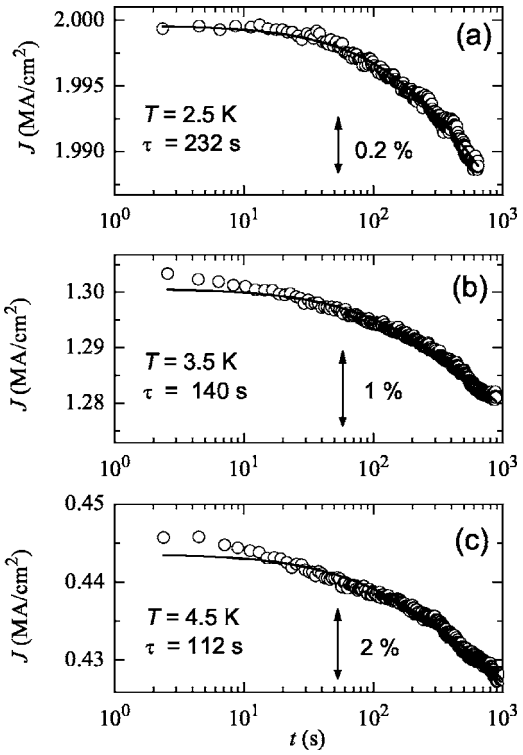

FIG. 14. Decay of the critical-current density vs time (log scale) for a 9 ML film with voids, measured in $H=5$ Oe dc field at (a) $T=2.5$ K, (b) $T=3.5$ K, and (c) $T=4.5$ K. Solid curves are fitted to Eq. (4) in the text. Markers show a fractional change in magnitude of the signal.

the Kim-Anderson framework of flux creep,[63,64] one has $S(T)=T/U_0(T)$. From the vortex pinning energy for single-vortex pinning,

$$U_0(T) = \varepsilon_0 \Delta d \propto \frac{1}{\lambda^2(T)} \propto \left[1 - \left(\frac{T}{T_c}\right)^2\right], \tag{8}$$

we finally obtain

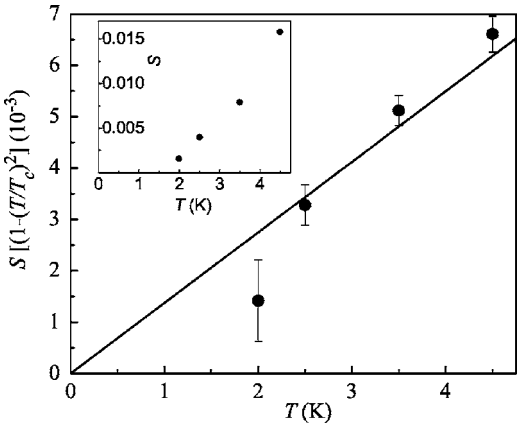

FIG. 15. The normalized creep rate S as corrected for the temperature dependence of vortex energy ε_0 plotted vs temperature. Plotted quantity demonstrates the temperature dependence of the creep rate in the Kim-Anderson formulation for a 9 ML film with voids ($H=5$ Oe). The inset shows the measured creep rate S, which is quite low.

$$S\left[1-\left(\frac{T}{T_c}\right)^2\right]=\frac{T}{U_0(T=0)}. \quad (9)$$

A plot of this quantity versus temperature in Fig. 15 reveals a reasonably linear dependence, thus supporting this analysis and yielding $U_0(T=0)\cong 700$ K. This result is in quite good agreement with the earlier *independent* estimate $U_0=\varepsilon_0\Delta d\sim 500$ K. Within our resolution, quantum tunneling of vortices does not seem to play a role in our system, as this would imply a nonzero creep rate S as $T\rightarrow 0$. Attempts to perform similar "stationary sample" creep measurements on a film with mesas were unsuccessful even at 5 Oe, due to the lower values of J_c and $5\times$ smaller superconductive signals that became lost in the drift and low-level instability of the measurement system. Overall, these "flux creep" results are consistent with the findings of the ac response study, that the ultrathin Pb films with voids exhibit strong vortex pinning and robust critical-state behavior.

IV. CONCLUDING REMARKS

In summary, superconductivity in atomically flat, quantum confined Pb films is unexpectedly robust against superconducting fluctuations and pair-breaking mechanisms that are usually associated with disorder and screening in reduced dimensionality. Superconductivity is controlled via a single parameter (thickness), which is varied with atomic precision. The film thickness directly affects T_c via the boundary conditions for the superconducting order parameter, while the superconductive length scales λ and ξ are affected via boundary scattering. The experiments provide an internally consistent set of parameters that semiquantitatively describe the thermodynamics and nonequilibrium response of the superconducting critical state. The power and validity of the 3D GL analysis for this extreme 2D geometry is perhaps the greatest surprise. This observation, however, may be rationalized on the basis of the time-energy uncertainty principle $\Delta E\geqslant\hbar\langle v_F\rangle l(d)^{-1}$ (v_F is the Fermi velocity). ΔE appears to be of the order of a few tenths of an eV, comparable to the intersubband spacing in quantum confined Pb, so that carriers can be scattered between 2D subbands. Strict 2D Cooper pairing thus requires long mean-free paths or, equivalently, a perfect interface between the film and the substrate.

ACKNOWLEDGMENTS

We wish to thank L. Bulaevskii, J. R. Clem, and A. Gurevich for useful discussions. This work has been funded primarily by the National Science Foundation under Contract No. DMR-0244570, and in part by the Division of Materials Sciences and Engineering, Office of Basic Energy Sciences, U.S. Department of Energy, under Contract No. DE-AC05-00OR22725 with Oak Ridge National Laboratory, managed and operated by UT-Battelle, LLC.

[1] A. Yazdani and A. Kapitulnik, Phys. Rev. Lett. **74**, 3037 (1995).
[2] A. M. Goldman and N. Marković, Phys. Today **11**, 39 (1998).
[3] A. Bezryadin, C. N. Lau, and M. Tinkham, Nature (London) **404**, 971 (2000).
[4] M. Zgirski, K.-P. Riikonen, V. Toubolotsev, and K. Arutyunov, Nano Lett. **5**, 1029 (2005).
[5] M. Hermele, G. Refael, M. P. A. Fisher, and P. M. Goldbart, Nat. Phys. **1**, 117 (2005).
[6] M. R. Beasley, J. E. Mooij, and T. P. Orlando, Phys. Rev. Lett. **42**, 1165 (1979).
[7] J. M. Kosterlitz and D. J. Thouless, J. Phys. C **6**, 1181 (1973).
[8] V. L. Berezinskii, Sov. Phys. JETP **32**, 493 (1970); **34**, 610 (1971).
[9] G. Blatter, M. V. Feigel'man, V. B. Geshkenbein, A. I. Larkin, and V. M. Vinokur, Rev. Mod. Phys. **66**, 1125 (1994).
[10] J. M. Graybeal and M. R. Beasley, Phys. Rev. B **29**, 4167 (1984).
[11] A. E. White, R. C. Dynes, and J. P. Garno, Phys. Rev. B **33**, 3549 (1986).
[12] J. M. Valles, Jr., R. C. Dynes, and J. P. Garno, Phys. Rev. B **40**, 6680 (1989).
[13] D. B. Haviland, Y. Liu, and A. M. Goldman, Phys. Rev. Lett. **62**, 2180 (1989).
[14] S. J. Lee and J. B. Ketterson, Phys. Rev. Lett. **64**, 3078 (1990).
[15] J. W. P. Hsu and A. Kapitulnik, Phys. Rev. B **45**, 4819 (1992).
[16] J. A. Chervenak and J. M. Valles, Jr., Phys. Rev. B **59**, 11209 (1999).
[17] T. R. Kirkpatrick and D. Belitz, Phys. Rev. Lett. **68**, 3232 (1992).
[18] M. A. Skvortsov and M. V. Feigel'man, Phys. Rev. Lett. **95**, 057002 (2005).
[19] M. M. Özer, J. R. Thompson, and H. H. Weitering, Nat. Phys. **2**, 173 (2006).
[20] Z. Zhang, Q. Niu, and C.-K. Shih, Phys. Rev. Lett. **80**, 5381 (1998).
[21] K. Budde, E. Abram, V. Yeh, and M. C. Tringides, Phys. Rev. B **61**, (R)10602 (2000).
[22] M. M. Özer, Y. Jia, B. Wu, Z. Zhang, and H. H. Weitering, Phys. Rev. B **72**, 113409 (2005).
[23] W. B. Su, S. H. Chang, W. B. Jian, C. S. Chang, L. J. Chen, and Tien T. Tsong, Phys. Rev. Lett. **86**, 5116 (2001).
[24] H. Okamoto, D. Chen, and T. Yamada, Phys. Rev. Lett. **89**, 256101 (2002).
[25] M. H. Upton, C. M. Wei, M. Y. Chou, T. Miller, and T.-C. Chiang, Phys. Rev. Lett. **93**, 026802 (2004).
[26] Y. Guo, Y.-F. Zhang, X.-Y. Bao, T.-Z. Han, Z. Tang, L.-X. Zhang, W.-G. Zhu, E. G. Wang, Q. Niu, Z. Q. Qiu, J.-F. Jia, Z.-X. Zhao, and Q.-K. Xue, Science **306**, 1915 (2004).
[27] D. Eom, S. Qin, M. Y. Chou, and C. K. Shih, Phys. Rev. Lett. **96**, 027005 (2006).
[28] J. Pearl, Appl. Phys. Lett. **5**, 65 (1964).
[29] M. Tinkham, *Introduction to Superconductivity* (Dover Publications Inc., Mineola, NY, 1996).
[30] R. Feng, E. H. Conrad, M. C. Tringides, C. Kim, and P. F. Miceli, Appl. Phys. Lett. **85**, 3866 (2004).
[31] A. Mans, J. H. Dil, A. R. H. F. Ettema, and H. H. Weitering, Phys. Rev. B **66**, 195410 (2002).
[32] J. R. Clem and A. Sanchez, Phys. Rev. B **50**, 9355 (1994).

[33] A. A. Abrikosov and L. P. Gor'kov, Zh. Eksp. Teor. Fiz. **35**, 1558 (1958); **36**, 319 (1959) [Sov. Phys. JETP **8**, 1090 (1959) **9**, 220 (1959)].
[34] A. A. Abrikosov, Rev. Mod. Phys. **76**, 975 (2004).
[35] G. J. Dolan and J. Silcox, Phys. Rev. Lett. **30**, 603 (1973).
[36] Xin-Yu Bao, Yan-Feng Zhang, Yupeng Wang, Jin-Feng Jia, Qi-Kun Xue, X. C. Xie, and Zhong-Xian Zhao, Phys. Rev. Lett. **95**, 247005 (2005).
[37] A. M. Finkel'stein, Pis'ma Zh. Eksp. Teor. Fiz. **45**, 37 (1987);[JETP Lett. **45**, 46 (1987)].
[38] S. Maekawa and H. Fukuyama, J. Phys. Soc. Jpn. **51**, 1380 (1981).
[39] M. Strongin, R. S. Thompson, O. F. Kammerer, and J. E. Crow, Phys. Rev. B **1**, 1078 (1970); the $\rho \times l$, product in Ref. 40 is slightly smaller ($\rho \times l = 1.1 \times 10^{-11}\ \Omega\,\mathrm{cm}^2$), which would imply that the $R_\square$ of the 5 ML film could even be lower ($\sim 150\ \Omega$).
[40] I. Vilfan, M. Henzler, O. Pfennigstorf, and H. Pfnür, Phys. Rev. B **66**, 241306(R) (2002).
[41] J. Simonín, Phys. Rev. B **33**, 7830 (1986).
[42] S. Takahashi and M. Tachiki, Phys. Rev. B **33**, 4620 (1986).
[43] V. M. Gvozdikov, Low Temp. Phys. **25**, 936 (1999).
[44] L. N. Bulaevskiĭ, V. L. Ginzburg, and A. A. Sobyanin, Sov. Phys. JETP **68**, 1499 (1988).
[45] D. S. Fisher, Phys. Rev. B **22**, 1190 (1980).
[46] Y. C. Kim, J. R. Thompson, J. G. Ossandon, D. K. Christen, and M. Paranthaman, Phys. Rev. B **51**, 11767 (1995).
[47] K. Maki, Ann. Phys. **34**, 363 (1965).
[48] T. P. Orlando, E. J. McNiff, Jr., S. Foner, and M. R. Beasley, Phys. Rev. B **19**, 4545 (1979).
[49] P. W. Anderson, J. Phys. Chem. Solids **11**, 26 (1959).
[50] F. Tafuri, J. R. Kirtley, D. Born, D. Stornaiuolo, P. G. Medaglia, P. Orgiani, G. Balestrino, and V. G. Kogan, Europhys. Lett. **73**, 948 (2006).
[51] Y. Jia, B. Wu, H. H. Weitering, and Z. Zhang, Phys. Rev. B **74**, 035433 (2005).
[52] C. P. Bean, Phys. Rev. Lett. **8**, 250 (1962).
[53] D. R. Nelson and V. M. Vinokur, Phys. Rev. B **48**, 13060 (1993).
[54] G. S. Mkrtchyan and V. V. Shmidt, Sov. Phys. JETP **34**, 195 (1972).
[55] E. H. Brandt, Phys. Rev. B **55**, 14513 (1997).
[56] D. V. Shantsev, Y. M. Galperin, and T. H. Johansen, Phys. Rev. B **61**, 9699 (2000).
[57] A. M. Campbell and J. E. Evetts, Adv. Phys. **50**, 1249 (2001);[reprinted from **21**, 199 (1972)].
[58] G. Pasquini, L. Civale, H. Lanza, and G. Nieva, Phys. Rev. B **65**, 214517 (2002).
[59] Th. Herzog, H. A. Radovan, P. Ziemann, and E. H. Brandt, Phys. Rev. B **56**, 2871 (1997).
[60] J. R. Thompson, K. D. Sorge, C. Cantoni, H. R. Kerchner, D. K. Christen, and M. Paranthaman, Supercond. Sci. Technol. **18**, 970 (2005).
[61] A. Gurevich and E. H. Brandt, Phys. Rev. Lett. **73**, 178 (1994).
[62] H. Yamasaki, Y. Nakagawa, Y. Mawatari, and B. Cao, Physica C **273**, 213 (1997).
[63] P. W. Anderson, Phys. Rev. Lett. **9**, 309 (1962).
[64] P. W. Anderson and Y. B. Kim, Rev. Mod. Phys. **36**, 39 (1964).